A Journal of the Gesellschaft Deutscher Chemiker

Angewandte International Edition GDCh Chemie

www.angewandte.org

Accepted Article

Title: Photo-Induced Ruthenium-Catalyzed C–H Arylation at Ambient Temperature

Authors: Korkit Korvorapun, Julia Struwe, Agnese Zangarelli, Rositha Kuniyil, Anna Casnati, Marjo Waeterschoot, and Lutz Ackermann

This manuscript has been accepted after peer review and appears as an Accepted Article online prior to editing, proofing, and formal publication of the final Version of Record (VoR). This work is currently citable by using the Digital Object Identifier (DOI) given below. The VoR will be published online in Early View as soon as possible and may be different to this Accepted Article as a result of editing. Readers should obtain the VoR from the journal website shown below when it is published to ensure accuracy of information. The authors are responsible for the content of this Accepted Article.

To be cited as: *Angew. Chem. Int. Ed.* 10.1002/anie.202003035

Link to VoR: https://doi.org/10.1002/anie.202003035

WILEY-VCH

10.1002/anie.202003035

WILEY-VCH

RESEARCH ARTICLE

Photo-Induced Ruthenium-Catalyzed C–H Arylations at Ambient Temperature

Korkit Korvorapun[+], Julia Struwe[+], Rositha Kuniyil, Agnese Zangarelli, Anna Casnati, Marjo Waeterschoot, and Lutz Ackermann*

Dedicated to Professor Rolf Huisgen on the occasion of his 100th birthday

Abstract: Ambient temperature ruthenium-catalyzed C–H arylations were accomplished by visible light without additional photocatalysts. The robustness of the ruthenium-catalyzed C–H functionalization protocol was reflected by a broad range of sensitive functional groups and synthetically useful pyrazoles, triazoles and sensitive nucleosides and nucleotides, as well as multifold C–H functionalizations. Biscyclometalated ruthenium complexes were identified as the key intermediates in the photoredox ruthenium catalysis by detailed computational and experimental mechanistic analysis. Calculations suggested that the in-situ formed photoactive ruthenium species preferably underwent an inner-sphere electron transfer.

Introduction

During the recent decade, transition metal-catalyzed C–H functionalizations have emerged as a powerful tool in molecular syntheses[1] with notable advances by ruthenium catalysis.[2] Particularly, C–H arylations[3] have played an important role in material sciences, crop protection, and drug discovery.[4] Ruthenium-catalyzed C–H arylations have hence been exploited for the synthesis of biologically active compounds, such as Anacetrapib, Valsartan, and Candesartan by Ouellet at Merck,[5] Ackermann,[6] and Seki,[7] respectively (Figure 1a). In addition, ruthenium-catalyzed C–H arylations have enabled late-stage peptide[8] and nucleoside functionalizations.[9]

Despite of major advances, ruthenium-catalyzed C–H arylations continue to be restricted to high reaction temperatures of typically 100–140 °C (Figure 1b).[10] The mechanism for ruthenium-catalyzed direct arylations with haloarenes was thus far generally accepted to occur through a ruthenium(II/IV) pathway by oxidative addition and reductive elimination.[10k]

Visible-light photoredox catalysis[11] allowed for direct transformations at ambient temperature, however, additional iridium[12] or ruthenium[13] photocatalysts were required in these transformations among others as reported by MacMillan, Molander and Doyle. In contrast, Ackermann[14] and Greaney[15] recently disclosed photo-induced ruthenium-catalyzed remote C–H alkylations. After submission of the present manuscript, Greaney has reported on a ruthenium-catalyzed arylation of phenylpyridines using visible light, which was proposed to occur by an oxidative addition/reductive elimination process.[16] Within our program on sustainable C–H activation,[17] we have now devised the first light-driven ruthenium-catalyzed C–H arylations at ambient temperature (Figure 1c). Notable features of our strategy include (i) a versatile dual-functional ruthenium(II) biscarboxylate catalyst for selective direct arylations, (ii) visible-light-induced C–H activation, (iii) photocatalysts-free ambient temperature transformations, (iv) versatile C–H arylations on transformable arenes and biorelevant purines, and (v) mechanistic insights by experiment and computation, being supportive of a ruthenium(II/III/IV) mechanism.

[*] K. Korvorapun,[+] J. Struwe,[+] Dr. R. Kuniyil, A. Zangarelli, A. Casnati, M. Waeterschoot, Prof. Dr. L. Ackermann
Institut für Organische und Biomolekulare Chemie
Georg-August-Universität Göttingen
Tammannstrasse 2, 37077 Göttingen (Germany)
E-mail: Lutz.Ackermann@chemie.uni-goettingen.de
Homepage: http://www.ackermann.chemie.uni-goettingen.de/

[+] These authors contributed equally to this work.

Supporting information for this article is given via a link at the end of the document.((Please delete this text if not appropriate))

Accepted Manuscript

This article is protected by copyright. All rights reserved.

10.1002/anie.202003035
WILEY-VCH

RESEARCH ARTICLE

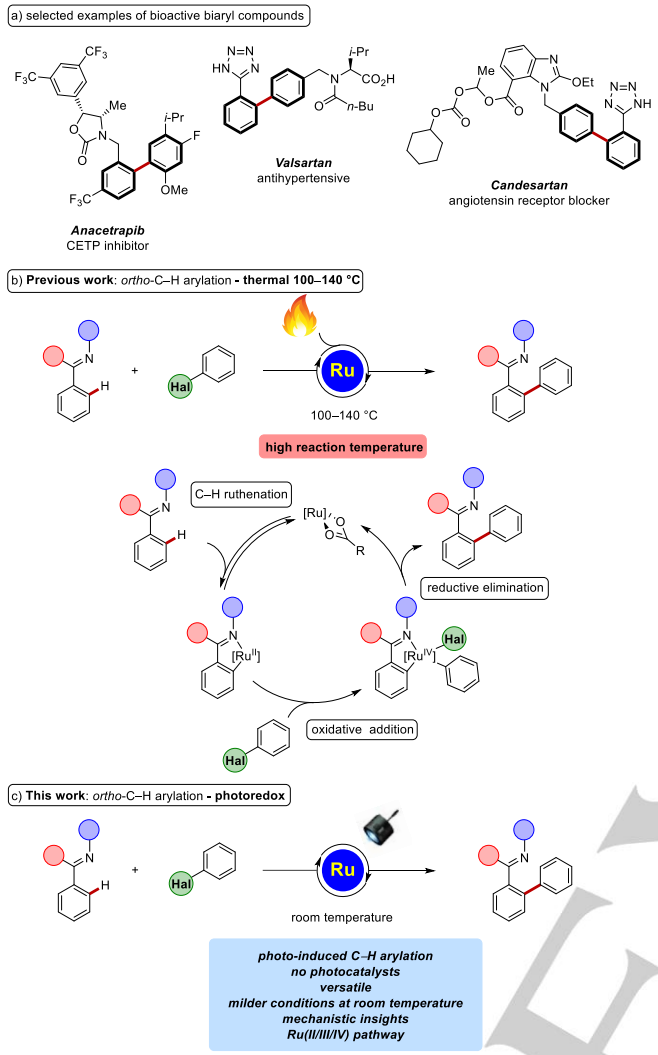

Figure 1. (a) Bioactive biaryls and ruthenium-catalyzed C–H arylations: (b) under thermal reaction condition and (c) under photoredox condition.

Results and Discussion

We commenced our studies by probing various reaction conditions for the envisioned C–H arylations of arene **1a** with 4-iodoanisole (**2a**) (Table 1).[18] Carboxylate assistance[19] was found to be key to achieve the *ortho*-C–H arylation (entries 1–4). Specifically, we found that [Ru(OAc)$_2$(*p*-cymene)] (**4**) in 1,4-dioxane was the most effective catalyst (entry 1). Cationic ruthenium(II) complexes in DMA as the solvent also provided the *ortho*-arylated product **3aa**, albeit only in moderate yield (entries 5–6). Other ruthenium sources, such as $Ru_3(CO)_{12}$ and $RuCl_3{\cdot}nH_2O$, failed to give the desired product **3aa** (entry 7). Control experiments verified the essential role of the ruthenium catalyst (entry 8), the base (entry 9), and the blue light (entry 10). In the dark, the reaction was sluggish even at a reaction temperature of 100 °C, reflecting the great influence of visible light on the C–H arylation. In addition, aryl bromides, chlorides, and triflates also furnished the corresponding product **3aa** in good yields (entry 11).[18] While thermal C–H arylations had been realized with different halides by a ruthenium(II/IV) pathway,[10l] sustainable light energy allowed first ambient temperature arylations, being superior to thermal reactions even at 100 °C.

Table 1. Optimization of photo-induced ruthenium(II)-catalyzed C–H arylation

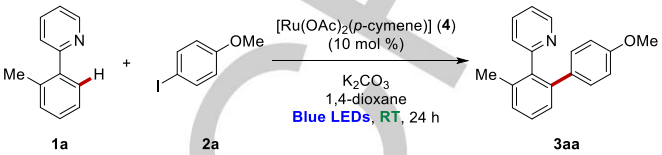

Entry	Deviation from the standard conditions	Yield [%][a]
1	none	94
2	$[RuCl_2(p\text{-cymene})]_2$ instead of **4**	(6)
3	$[RuCl_2(p\text{-cymene})]_2$ instead of **4** and KOAc instead of K_2CO_3	90
4	*n*-Bu_4NOAc instead of K_2CO_3	78
5	$[Ru(NCt\text{-}Bu)_6][PF_6]_2$ instead of **4** and $MesCO_2H$ (30 mol %) as the additive	(4)
6	$[Ru(NCt\text{-}Bu)_6][PF_6]_2$ instead of **4** and $MesCO_2H$ (30 mol %) as the additive, DMA instead of 1,4-dioxane	(52)
7	$Ru_3(CO)_{12}$, $RuCl_3{\cdot}nH_2O$ instead of **4** and $MesCO_2H$ (30 mol %) as the additive	(0), (0)
8	no [Ru], at 30–35 °C	(0)
9	no K_2CO_3, at 30–35 °C	(14)
10	no light, at 30–35, 40, 60, 80, 100 °C	(12), (9), (15), (32), (49)
11	ArBr, ArCl, ArOTf instead of ArI	68, (43), 39

[a] Reaction conditions: **1a** (0.50 mmol), ArI **2a** (0.75 mmol), [Ru(OAc)$_2$(*p*-cymene)] (10 mol %), K_2CO_3 (1.00 mmol), 1,4-dioxane (2.0 mL), 30–35 °C, 24 h, under N_2, blue LEDs; yield of isolated products. The yield in the parentheses were determined by ^{1}H-NMR spectroscopy using 1,3,5-trimethoxybenzene as the internal standard.

With the optimized reaction conditions in hand, we probed its versatility in the direct C–H arylation of 2-arylpyridine **1a** and a variety of aryl iodides **2** (Scheme 1). Electron-donating and electron-withdrawing groups of *para*- and *meta*-substituted aryl halides were well tolerated, affording the corresponding arylated product **3** with moderate to high efficacy. Sterically hindered 2-iodoanisole (**2s**) also delivered the desired product **3as**. It is noteworthy that the ruthenium-catalyzed C–H arylation proved widely applicable, tolerating sensitive functional groups, including hydroxyl (**3af**), chloro, bromo (**3ah**–**3ai**), ketone (**3ak** and **3aq**), ester (**3al**) and nitrile (**3ar**). In addition, the ruthenium(II) catalysis was effective for (*NH*)-free indole (**3aw**) and carbazole (**3az**).[20] Besides monohaloarenes, the room temperature ruthenium catalysis regime proved applicable to the twofold (**5aa'**–**5ac'**)[20] or threefold C–H functionalization (**5ad'**).

Accepted Manuscript

This article is protected by copyright. All rights reserved.

10.1002/anie.202003035

WILEY-VCH

RESEARCH ARTICLE

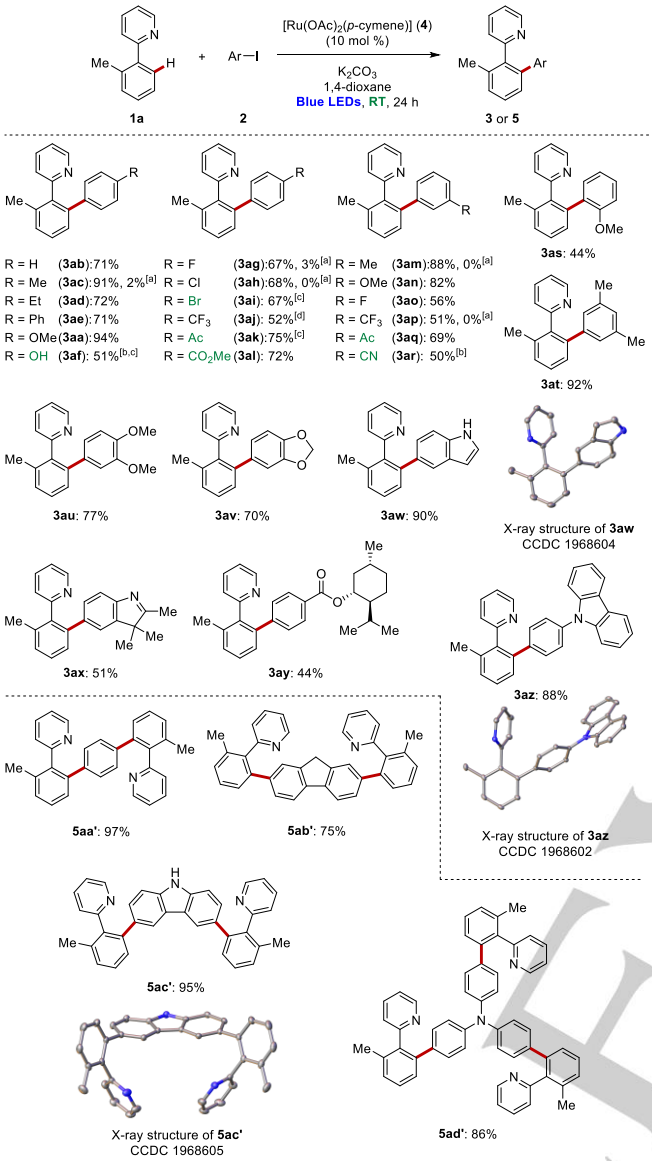

Scheme 1. Photo-induced ruthenium(II)-catalyzed C–H arylation at ambient temperature. [a] No light at 30–35 °C. [b] DMA as solvent. [c] 48 h. [d] 4-Bromobenzotrifluoride.

The C–H arylation was not restricted to the assistance by pyridines. Indeed, arenes bearing pyrimidines **1e**, transformable imidates **1f**–**1g**, and removable pyrazoles **1h**–**1j** were efficiently converted into the desired products **3** (Scheme 2a).[20] In addition, ketimine **1k** underwent the photo-induced arylation followed by acidic hydrolysis to afford the *ortho*-arylated acetophenone **3ka** (Scheme 2b).

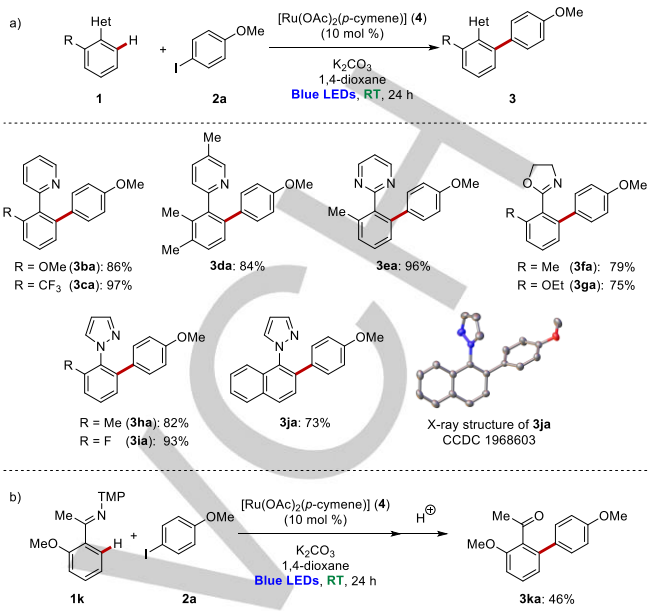

Scheme 2. Room-temperature visible-light-enabled ruthenium-catalyzed C–H arylation with a) heteroarenes **1** and b) ketimine **1k**. TMP = 3,4,5-trimethoxyphenyl.

Notably, the application of the room temperature direct arylation with substituted click-triazole[21] **1l** selectively provided the corresponding products **3la**, **3lg**, **3lv** (Scheme 3).

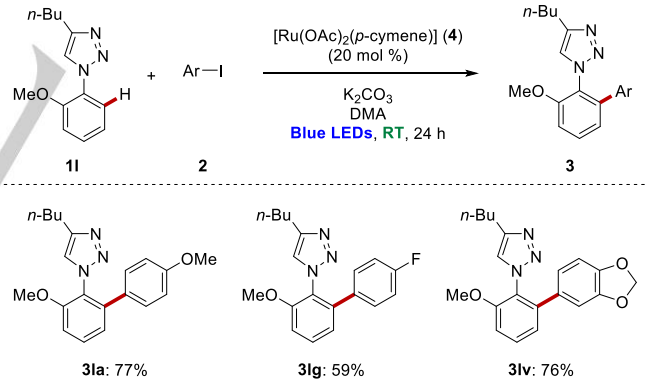

Scheme 3. Ruthenium-catalyzed C–H arylation with substituted click-triazole **1l**.

The unique potential of the direct photoredox arylation was mirrored by the improved chemo-selectivities in the reactions with 4-iodophenyl triflate (**2e'**) or 1-bromo-3-iodobenzene (**2f'**), predominantly affording the monoarylation products, while leaving the valuable electrophilic (pseudo)halides intact (Scheme 4a and 4b). In sharp contrast, the thermal reactions delivered the diarylated products **5**, lacking a discrimination of the complementary aryl halides. Furthermore, the light-induced C–H arylation of naphthyl-pyrazole **1j** with 2-bromo-5-iodotoluene (**2g'**) provided the desired monoarylated product **3jg'** (Scheme 4c). In stark contrast, undesired protodebromination was observed by conventional thermal arylations.

Accepted Manuscript

This article is protected by copyright. All rights reserved.

10.1002/anie.202003035

WILEY-VCH

RESEARCH ARTICLE

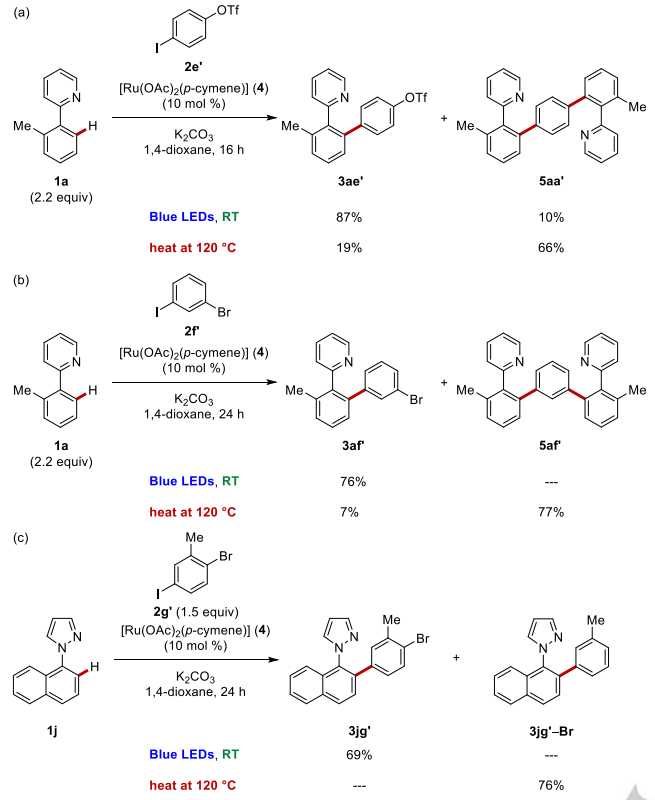

Scheme 4. Improved chemo-selectivity by visible-light-induced C–H arylation.

Given the synthetic utility of the mild photo-induced ruthenium(II)-catalyzed direct C–H arylations, we became attracted to delineating its mode of action. To this end, intermolecular competition experiments of *ortho*-substituted arenes **1** showed a minor electronic bias,[18] while experiments of *meta*-substituted arenes **1** highlighted electron-poor arenes to be more efficiently converted (Scheme 5a). Moreover, a significant amount of free *p*-cymene (**6**) was observed by decoordination from the ruthenium precatalyst (Scheme 5b). An arene-ligand-free ruthenacycle **7**, as previously exploited by Larrosa and our group,[3c, 22] was only effective in the presence of KOAc (Scheme 5c), which suggested that a carboxylate-modified ruthenacycle was involved in the photo-induced C–H arylation.

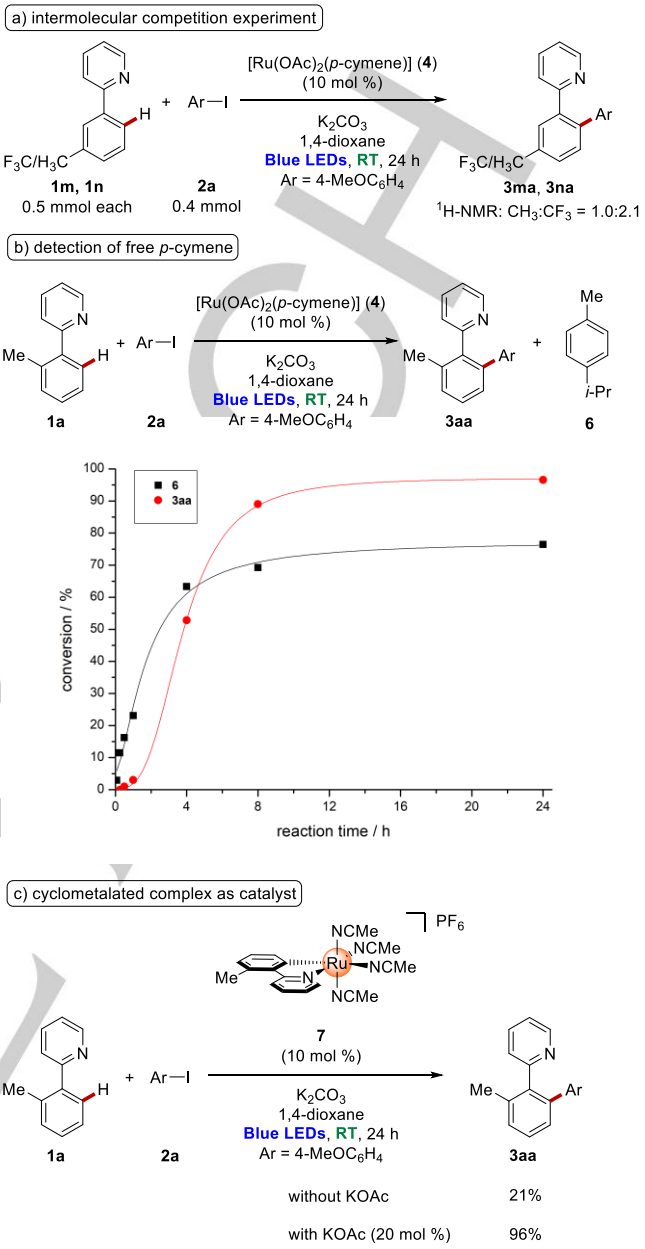

Scheme 5. Key mechanistic studies.

To elucidate the role of the blue light, we conducted an on/off light experiment (Figure 2).[18] The conversion of the direct *ortho*-arylation was completely suppressed in the absence of light, being indicative of the photo-induced ruthenium(II)-catalyzed arylation not involving a radical chain process. In addition, we obtained the quantum yield of Φ = 0.087 for the photoredox ruthenium-catalyzed arylation.[18]

Accepted Manuscript

This article is protected by copyright. All rights reserved.

10.1002/anie.202003035

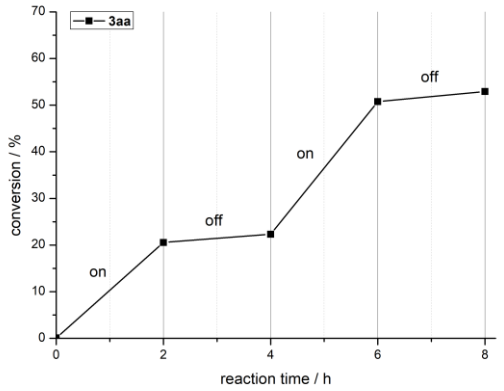

Figure 2. On/off light experiment.

In order to gain detailed insights into the reaction mechanism, DFT calculations were performed for biscyclometalated ruthenacycle enabled *ortho*-C–H arylations at the PBE0-D3(BJ)/6-311++G(d,p),def2-TZVP(Ru,I),SDD(Ru,I)+ SMD(1,4-dioxane)//B3LYP-D3(BJ)/6-31G(d),def2-SVP(Ru,I), SDD(Ru,I) level of theory.[18] Initially we studied the absorption properties[23] of the monocyclometalated ruthenacycles **8** and **9** as well as the biscyclometalated complexes **10** and **11** (Figure 3a). The TD-DFT calculations of complexes **10** and **11** confirmed the existence of a strong metal-to-ligand charge-transfer (MLCT) with a maximum absorption at λ = 461.44 (oscillator strength of 0.1810) and 461.41 nm (oscillator strength of 0.1601), respectively. These findings are in good agreement with an orbital analysis of complex **11** (Figure 3b). In sharp contrast, the monocyclometalated complexes **8** and **9** featured a maximum absorption band outside the visible-light range.

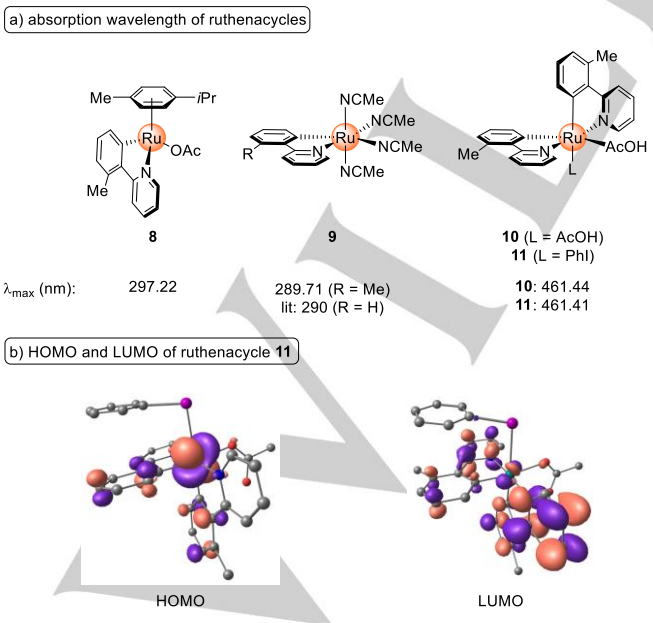

Figure 3. Computational analysis: a) absorption wavelength of mono- and biscyclometalated ruthenacycles, b) HOMO and LUMO of biscyclometalated ruthenium complex **11**.

On the basis of our findings, the complexes **10** and **11** were further studied for the photoredox arylations (Figure 4). The excitation of iodoarene-coordinated ruthenacycle complex **11** followed by intersystem crossing (ISC) leads to a long-lived triplet complex **11**** with an energy of 30.7 kcal·mol^{-1} as compared to the complex **10** (Figure 4a). Afterwards, inner-sphere electron transfer (ISET) to iodoarene occurs through a low barrier transition state **TS1** to form phenyl radical and ruthenium(III) intermediate **12**. The radical recombination of complex **12** affords a stable ruthenium(IV) intermediate **14**. Apart from the ISET process, we considered potentially viable outer-sphere electron transfer (OSET) from the triplet state **10**** to iodoarene molecule (Figure 4b). The OSET transition state **TS3** has a barrier of 63.1 kcal·mol^{-1}, as computed using Marcus theory[24] and Savéant's model,[25] and thereby generates cationic ruthenium complex **16** with an energy of 57.6 kcal·mol^{-1} as compared to the complex **10**. Therefore, the ISET mechanism is considered to be favorable over the OSET pathway.

Accepted Manuscript

This article is protected by copyright. All rights reserved.

10.1002/anie.202003035

WILEY-VCH

RESEARCH ARTICLE

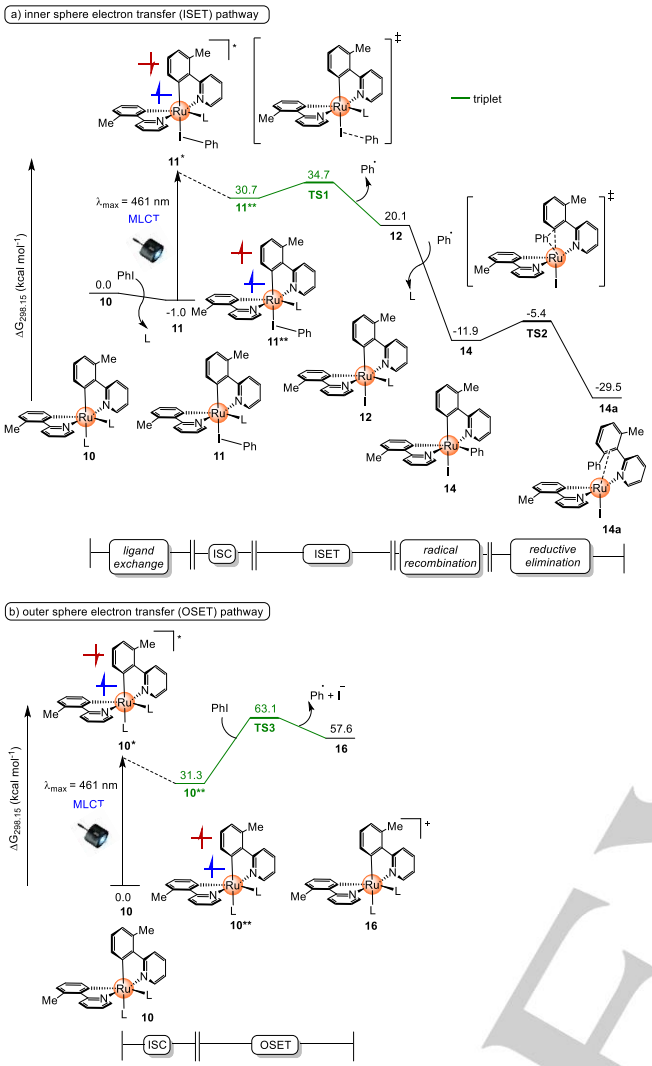

Figure 4. Relative Gibbs free energy profile in kcal mol^{-1} with respect to **10** at thePBE0-D3(BJ)/6-311++G(d,p),def2-TZVP(Ru,I),SDD(Ru,I)+ SMD(1,4dioxane)//B3LYP-D3(BJ)/6-31G(d),def2-SVP(Ru,I),SDD(Ru,I) level of theory for photo-induced ruthenium-catalyzed C–H arylation via a) inner-sphere electron transfer (ISET) and b) outer-sphere electron transfer (OSET) pathways. L = AcOH.

Based on our findings, a plausible catalytic cycle commences by carboxylate-assisted C–H ruthenation and dissociation of *p*-cymene,[22d] generating the corresponding biscyclometalated complex **10** (Scheme 6). The coordination of iodoarene to complex **10** leads to ruthenacycle **11**, which is excited by blue-light-absorption to form singlet excited species **11***. Relaxation through intersystem crossing (ISC) affords a long-lived triplet complex **11****. Subsequently, an inner-sphere electron transfer (ISET) to iodoarene generates a phenyl radical (**13**) and ruthenium(III) intermediate **12**. They readily recombine to form stable ruthenium(IV) intermediate **14**. Reductive elimination and ligand exchange deliver the arylated product **3** and ruthenium complex **15**, which finally undergoes C–H ruthenation to regenerate the photocatalytically active ruthenium(II) complex **10**.

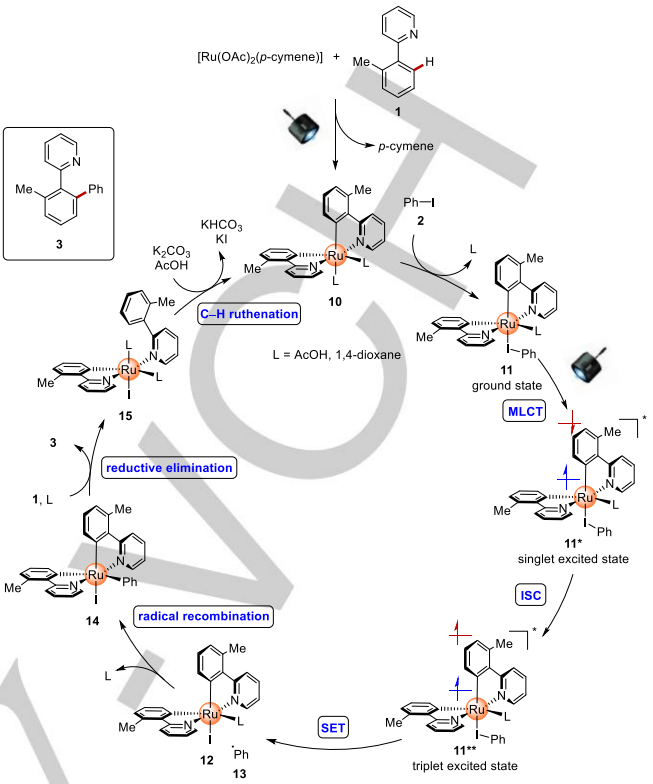

Scheme 6. Proposed catalytic cycle.

Finally, the power of the photo-induced ruthenium-catalyzed arylation at ambient temperature was highlighted by the late-stage diversification of biorelevant purines **1o**–**1p**, sensitive nucleoside **1q** and nucleotide **1r** (Scheme 7).

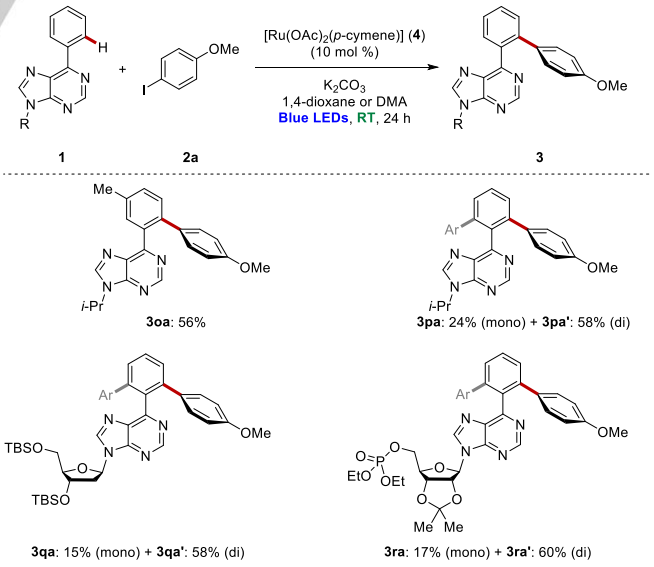

Scheme 7. Late-stage diversification: photo-induced ruthenium-catalyzed C–H arylation with biorelevant purines at room temperature.

Accepted Manuscript

This article is protected by copyright. All rights reserved.

Conclusion

In summary, we have reported on ambient temperature ruthenium-catalyzed C–H arylations enabled by visible light. The versatile photoredox ruthenium catalysis proved viable with a broad range of functional groups and applicable to synthetically useful pyrazoles, triazoles and sensitive nucleosides and nucleotides. Mechanistic studies by experiment and computation were suggestive of an inner-sphere electron transfer from photocatalytically active biscyclometalated ruthenacycles for the photoredox catalysis.

Acknowledgements

Generous support by the DAAD (fellowship to K.K.) and the DFG (Gottfried-Wilhelm-Leibniz prize) is gratefully acknowledged. We thank Dr. Christopher Golz (University Göttingen) for the X-ray diffraction analysis.

Keywords: C–H activation • photocatalysis • ruthenium • arylation • photochemistry

[1] a) S. Rej, Y. Ano, N. Chatani, *Chem. Rev.* **2020**, *120*, 1788-1887; b) P. Gandeepan, T. Müller, D. Zell, G. Cera, S. Warratz, L. Ackermann, *Chem. Rev.* **2019**, *119*, 2192–2452; c) Y. Hu, B. Zhou, C. Wang, *Acc. Chem. Res.* **2018**, *51*, 816–827; d) C. Sambiagio, D. Schönbauer, R. Blieck, T. Dao-Huy, G. Pototschnig, P. Schaaf, T. Wiesinger, M. F. Zia, J. Wencel-Delord, T. Besset, B. U. W. Maes, M. Schnürch, *Chem. Soc. Rev.* **2018**, *47*, 6603-6743; e) J. A. Leitch, C. G. Frost, *Synthesis* **2018**, *50*, 2693-2706; f) Y. Park, Y. Kim, S. Chang, *Chem. Rev.* **2017**, *117*, 9247–9301; g) Z. Huang, H. N. Lim, F. Mo, M. C. Young, G. Dong, *Chem. Soc. Rev.* **2015**, *44*, 7764-7786; h) K. Gao, N. Yoshikai, *Acc. Chem. Res.* **2014**, *47*, 1208–1219; i) J. Wencel-Delord, F. Glorius, *Nat. Chem.* **2013**, *5*, 369–375; j) K. M. Engle, T.-S. Mei, M. Wasa, J.-Q. Yu, *Acc. Chem. Res.* **2012**, *45*, 788-802; k) P. B. Arockiam, C. Bruneau, P. H. Dixneuf, *Chem. Rev.* **2012**, *112*, 5879–5918; l) L. Ackermann, R. Vicente, A. R. Kapdi, *Angew. Chem. Int. Ed.* **2009**, *48*, 9792–9826.

[2] a) K. Korvorapun, R. Kuniyil, L. Ackermann, *ACS Catal.* **2020**, *10*, 435–440; b) J. Li, K. Korvorapun, S. De Sarkar, T. Rogge, D. J. Burns, S. Warratz, L. Ackermann, *Nat. Commun.* **2017**, *8*, 15430; c) C. J. Teskey, A. Y. W. Lui, M. F. Greaney, *Angew. Chem. Int. Ed.* **2015**, *54*, 11677–11680; d) A. J. Paterson, S. St John-Campbell, M. F. Mahon, N. J. Press, C. G. Frost, *Chem. Commun.* **2015**, *51*, 12807–12810; e) L. Wang, L. Ackermann, *Chem. Commun.* **2014**, *50*, 1083–1085; f) G. Rouquet, N. Chatani, *Chem. Sci.* **2013**, *4*, 2201–2208; g) M. Schinkel, I. Marek, L. Ackermann, *Angew. Chem. Int. Ed.* **2013**, *52*, 3977–3980; h) L. Ackermann, P. Novák, R. Vicente, N. Hofmann, *Angew. Chem. Int. Ed.* **2009**, *48*, 6045–6048; i) S. Murai, F. Kakiuchi, S. Sekine, Y. Tanaka, A. Kamatani, M. Sonoda, N. Chatani, *Nature* **1993**, *366*, 529-531; j) L. N. Lewis, J. F. Smith, *J. Am. Chem. Soc.* **1986**, *108*, 2728-2735.

[3] a) T. Rogge, L. Ackermann, *Angew. Chem. Int. Ed.* **2019**, *58*, 15640-15645; b) S. R. Yetra, T. Rogge, S. Warratz, J. Struwe, W. Peng, P. Vana, L. Ackermann, *Angew. Chem. Int. Ed.* **2019**, *58*, 7490-7494; c) M. Simonetti, D. M. Cannas, X. Just-Baringo, I. J. Vitorica-Yrezabal, I. Larrosa, *Nat. Chem.* **2018**, *10*, 724-731; d) M. Moselage, J. Li, F. Kramm, L. Ackermann, *Angew. Chem. Int. Ed.* **2017**, *56*, 5341-5344; e) P. Nareddy, F. Jordan, M. Szostak, *ACS Catal.* **2017**, *7*, 5721-5745; f) M. Simonetti, D. M. Cannas, A. Panigrahi, S. Kujawa, M. Kryjewski, P. Xie, I. Larrosa, *Chem. Eur. J.* **2017**, *23*, 549-553; g) R. Mei, C. Zhu, L. Ackermann, *Chem. Commun.* **2016**, *52*, 13171-13174; h) M. Simonetti, G. J. P. Perry, X. C. Cambeiro, F. Juliá-Hernández, J. N. Arokianathar, I. Larrosa, *J. Am. Chem. Soc.* **2016**, *138*, 3596–3606; i) N. Y. P. Kumar, R. Jeyachandran, L. Ackermann, *J. Org. Chem.* **2013**, *78*, 4145-4152.

[4] a) L. Ackermann, *Org. Process Res. Dev.* **2015**, *19*, 260–269; b) D. A. Horton, G. T. Bourne, M. L. Smythe, *Chem. Rev.* **2003**, *103*, 893-930; c) J. Hassan, M. Sévignon, C. Gozzi, E. Schulz, M. Lemaire, *Chem. Rev.* **2002**, *102*, 1359-1470.

[5] S. G. Ouellet, A. Roy, C. Molinaro, R. Angelaud, J.-F. Marcoux, P. D. O'Shea, I. W. Davies, *J. Org. Chem.* **2011**, *76*, 1436-1439.

[6] a) J. Hubrich, L. Ackermann, *Eur. J. Org. Chem.* **2016**, *2016*, 3700-3704; b) E. Diers, N. Y. Phani Kumar, T. Mejuch, I. Marek, L. Ackermann, *Tetrahedron* **2013**, *69*, 4445-4453.

[7] M. Seki, *ACS Catal.* **2014**, *4*, 4047-4050.

[8] A. Schischko, H. Ren, N. Kaplaneris, L. Ackermann, *Angew. Chem. Int. Ed.* **2017**, *56*, 1576-1580.

[9] V. Gayakhe, Y. S. Sanghvi, I. J. S. Fairlamb, A. R. Kapdi, *Chem. Commun.* **2015**, *51*, 11944-11960.

[10] a) A. M. Spiewak, D. J. Weix, *J. Org. Chem.* **2019**, *84*, 15642-15647; b) J.-W. Li, L.-N. Wang, M. Li, P.-T. Tang, X.-P. Luo, M. Kurmoo, Y.-J. Liu, M.-H. Zeng, *Org. Lett.* **2019**, *21*, 2885-2889; c) R. Boyaala, R. Touzani, T. Roisnel, V. Dorcet, E. Caytan, D. Jacquemin, J. Boixel, V. Guerchais, H. Doucet, J.-F. Soulé, *ACS Catal.* **2019**, *9*, 1320-1328; d) M. Drev, U. Grošelj, B. Ledinek, F. Perdih, J. Svete, B. Štefane, F. Požgan, *Org. Lett.* **2018**, *20*, 5268-5273; e) F. Hu, M. Szostak, *Org. Lett.* **2016**, *18*, 4186–4189; f) J. Hubrich, T. Himmler, L. Rodefeld, L. Ackermann, *ACS Catal.* **2015**, *5*, 4089–4093; g) B. Li, C. Darcel, P. H. Dixneuf, *ChemCatChem* **2014**, *6*, 127-130; h) L. Ackermann, E. Diers, A. Manvar, *Org. Lett.* **2012**, *14*, 1154-1157; i) W. Li, P. B. Arockiam, C. Fischmeister, C. Bruneau, P. H. Dixneuf, *Green Chem.* **2011**, *13*, 2315-2319; j) L. Ackermann, A. V. Lygin, *Org. Lett.* **2011**, *13*, 3332-3335; k) L. Ackermann, R. Vicente, H. K. Potukuchi, V. Pirovano, *Org. Lett.* **2010**, *12*, 5032–5035; l) L. Ackermann, R. Vicente, A. Althammer, *Org. Lett.* **2008**, *10*, 2299-2302.

[11] For representative reviews, see: a) C.-S. Wang, P. H. Dixneuf, J.-F. Soulé, *Chem. Rev.* **2018**, *118*, 7532–7585; b) J. Twilton, C. Le, P. Zhang, M. H. Shaw, R. W. Evans, D. W. C. MacMillan, *Nat. Rev. Chem.* **2017**, *1*, 0052; c) D. C. Fabry, M. Rueping, *Acc. Chem. Res.* **2016**, *49*, 1969-1979; d) J. M. R. Narayanam, C. R. J. Stephenson, *Chem. Soc. Rev.* **2011**, *40*, 102-113.

[12] a) X. Zhang, D. W. C. MacMillan, *J. Am. Chem. Soc.* **2017**, *139*, 11353-11356; b) M. H. Shaw, V. W. Shurtleff, J. A. Terrett, J. D. Cuthbertson, D. W. C. MacMillan, *Science* **2016**, *352*, 1304-1308; c) D. R. Heitz, J. C. Tellis, G. A. Molander, *J. Am. Chem. Soc.* **2016**, *138*, 12715-12718; d) J. D. Cuthbertson, D. W. C. MacMillan, *Nature* **2015**, *519*, 74-77.

[13] a) P. Natarajan, N. Kumar, M. Sharma, *Org. Chem. Front.* **2016**, *3*, 1265-1270; b) D. Kalyani, K. B. McMurtrey, S. R. Neufeldt, M. S. Sanford, *J. Am. Chem. Soc.* **2011**, *133*, 18566-18569; c) M. Osawa, H. Nagai, M. Akita, *Dalton Trans.* **2007**, 827-829.

[14] P. Gandeepan, J. Koeller, K. Korvorapun, J. Mohr, L. Ackermann, *Angew. Chem. Int. Ed.* **2019**, *58*, 9820–9825.

[15] A. Sagadevan, M. F. Greaney, *Angew. Chem. Int. Ed.* **2019**, *58*, 9826–9830.

[16] A. Sagadevan, A. Charitou, F. Wang, M. Ivanova, M. Vuagnat, M. F. Greaney, *Chem. Sci.* **2020**,*11*, 4439–4443.

[17] a) L. Ackermann, *Acc. Chem. Res.* **2020**, *53*, 84-104; b) L. Ackermann, *Acc. Chem. Res.* **2014**, *47*, 281–295.

[18] For detailed information, see the Supporting Information.

[19] L. Ackermann, *Chem. Rev.* **2011**, *111*, 1315−1345.

[20] CCDC 1968604 (**3aw**), 1968602 (**3az**), 1968605 (**5ac'**), and 1968603 (**3ja**) contain the supplementary crystallographic data for this paper. These data can be obtained free of charge from The Cambridge Crystallographic Data Centre.

[21] a) L. Ackermann, H. K. Potukuchi, *Org. Biomol. Chem.* **2010**, *8*, 4503-4513; b) M. Meldal, C. W. Tornøe, *Chem. Rev.* **2008**, *108*, 2952-3015; c) H. C. Kolb, M. G. Finn, K. B. Sharpless, *Angew. Chem. Int. Ed.* **2001**, *40*, 2004-2021; d) R. Huisgen, *Angew. Chem. Int. Ed.* **1963**, *2*, 565-598.

[22] a) M. Simonetti, R. Kuniyil, S. A. Macgregor, I. Larrosa, *J. Am. Chem. Soc.* **2018**, *140*, 11836-11847; b) M. Simonetti, G. J. P. Perry, X. C. Cambeiro, F. Juliá-Hernández, J. N. Arokianathar, I. Larrosa, *J. Am. Chem. Soc.* **2016**, *138*, 3596-3606; c) L. Ackermann, A. Althammer, R. Born, *Tetrahedron* **2008**, *64*, 6115–6124; d) L. Ackermann, A. Althammer, R. Born, *Synlett* **2007**, 2833–2836; see also: e) S. Fernandez, M. Pfeffer, V. Ritleng, C. Sirlin, *Organometallics* **1999**, *18*, 2390-2394.

[23] A. D. Ryabov, H. Estevez, L. Alexandrova, M. Pfeffer, R. L. Lagadec, *Inorganica Chim. Acta* **2006**, *359*, 883–887.

[24] a) R. A. Marcus, *Angew. Chem. Int. Ed.* **1993**, *32*, 1111-1121; b) R. A. Marcus, *J. Chem. Phys.* **1956**, *24*, 966-978.

[25] a) J. M. Saveant, *Acc. Chem. Res.* **1993**, *26*, 455-461; b) J. M. Saveant, *J. Am. Chem. Soc.* **1987**, *109*, 6788-6795.

Accepted Manuscript

This article is protected by copyright. All rights reserved.

10.1002/anie.202003035

WILEY-VCH

RESEARCH ARTICLE

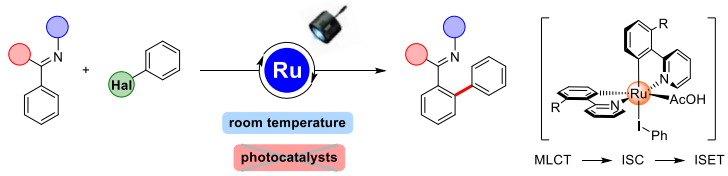

Light-enabled ruthenium-catalyzed C–H activation allowed for direct arylations at ambient temperature. Biscyclometalated ruthenium intermediates were identified as photoredox catalyst through a metal-to-ligand charge transfer (MLCT), intersystem crossing (ISC) and inner-sphere electron transfer (ISET) manifold.

*K. Korvorapun, J. Struwe, R. Kuniyil, A. Zangarelli, A. Casnati, M. Waeterschoot, L. Ackermann**

Page No. – Page No.

Photo-Induced Ruthenium-Catalyzed C–H Arylation at Ambient Temperature

WILEY-VCH

Accepted Manuscript

This article is protected by copyright. All rights reserved.